Absence of intrinsic ferromagnetism in $Zn_{1-x}Mn_xO$ alloys

2006 J. Phys.: Condens. Matter 18 L477

(http://iopscience.iop.org/0953-8984/18/39/L02)

INSTITUTE OF PHYSICS PUBLISHING JOURNAL OF PHYSICS: CONDENSED MATTER

J. Phys.: Condens. Matter **18** (2006) L477–L483 doi:10.1088/0953-8984/18/39/L02

LETTER TO THE EDITOR

Absence of intrinsic ferromagnetism in $Zn_{1-x}Mn_xO$ alloys

Hua-Wei Zhang[1,2], Er-Wei Shi[1], Zhi-Zhan Chen[1,3], Xue-Chao Liu[1,2] and Bing Xiao[1]

[1] Shanghai Institute of Ceramics, Chinese Academy of Sciences, Shanghai 200050, People's Republic of China
[2] Graduate School of the Chinese Academy of Sciences, Beijing 100049, People's Republic of China

E-mail: zzchen@mail.sic.ac.cn

Received 22 March 2006, in final form 31 August 2006
Published 15 September 2006
Online at stacks.iop.org/JPhysCM/18/L477

Abstract

$Zn_{1-x}Mn_xO$ alloys, with different Mn concentrations, were prepared by the hydrothermal method. X-ray diffraction and electron paramagnetic resonance spectra demonstrate that Zn^{2+} ions are homogeneously substituted by Mn^{2+} ions without changing the ZnO wurtzite structure. The $x = 0.02$ and 0.04 samples are paramagnetic. When the Mn concentrations are increased to $x = 0.08$ and 0.10, the samples exhibit some ferromagnetism due to a secondary phase, (Zn, Mn)Mn_2O_4.

1. Introduction

Diluted magnetic semiconductors (DMSs) have attracted a great deal of attention in recent years because of the possibility of incorporating the magnetic degrees of freedom into traditional semiconductor technologies [1–3]. After theoretical work [4] predicting the existence of high-temperature ferromagnetism (FM) in some magnetically doped wide band gap semiconductors, much attention has been paid to these materials. Among them, TiO_2 and ZnO doped with different transition metals (TM) have been the subject of intense research. In spite of the large number of papers published, the origin of ferromagnetism has not yet been elucidated definitively [5]. For Co-doped TiO_2, early results seemed to indicate the existence of intrinsic FM [6], but more recent works suggested that the segregation and formation of Co-doped anatase nanoscale particles are the origin of the FM signal [7]. Similarly, confusing results have also been reported on the Mn-doped ZnO system [8–10]. The controversies over these materials spur us on to the nature of the magnetism of DMSs.

In this contribution, we report on the magnetic states of $Zn_{1-x}Mn_xO$ alloys with different Mn concentrations. The samples with lower Mn concentrations are paramagnetic, while the

[3] Author to whom any correspondence should be addressed.

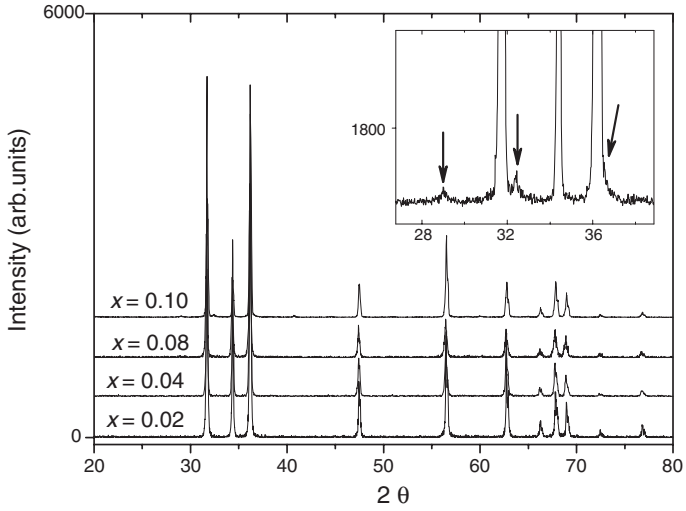

Figure 1. XRD patterns for the $Zn_{1-x}Mn_xO$ alloys prepared by the hydrothermal method. All the diffraction peaks belong to the hexagonal structure of ZnO for samples of $x = 0.02, 0.04$ and 0.08. The inset shows peaks due to a secondary phase in the $x = 0.10$ sample (labelled by arrows).

samples with higher Mn concentrations are ferromagnetic. However, the ferromagnetism is induced by a secondary phase.

2. Experiment

$Zn_{1-x}Mn_xO$ alloys were synthesized by a hydrothermal technique [11]. A platinum-lined stainless-steel autoclave was used. Compared to other chemical methods, the hydrothermal reaction proceeds at high temperature and pressure, which provides sufficient thermal energy to incorporate Mn^{2+} ions into the ZnO lattice. The raw material ZnO (99.99%) and $MnCl_2{\cdot}4H_2O$ (99.99%), in appropriate molar ratios, were first dissolved in 10 ml KOH solution. The solution was transferred into the autoclave, and then hydrothermally treated at 703 K for 24 h. After hydrothermal reaction, the precipitate was filtered, washed with distilled water several times and dried at 353 K. The phase was identified by x-ray diffraction (XRD, Rigaku D/MAX-2200). Scanning electron microscopy (SEM, EPMA-8705QH2) equipped with an energy dispersive spectrometer (EDAX) and transmission electron microscopy (TEM, JEOL 2100F) equipped with selected area electron diffraction (SAED) were used for micro-structural observations. The electron paramagnetic resonance (EPR, ESR300E) was performed, at X band frequencies (9.8 GHz) with a microwave power of 5 mW at 295 K, to determine whether the Mn^{2+} ions were incorporated into the ZnO lattice. Magnetic measurements were performed using a commercial superconducting quantum interference device (SQUID) magnetometer (Quantum Design MPMS, XL-7).

3. Results and discussion

The as-grown $Zn_{1-x}Mn_xO$ alloys were red and the colour became deep red with an increase in Mn concentration. The crystallite size was distributed from 3 to 30 μm for all samples. EDAX measurements revealed that x was 0.02, 0.04, 0.08 and 0.10, consistent with the sample fabrication procedure. Figure 1 illustrates the XRD patterns. The $x = 0.02$, 0.04 and 0.08

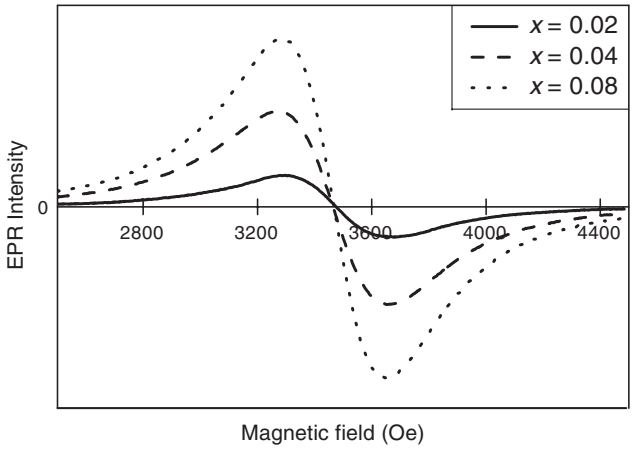

Figure 2. EPR spectra of $Zn_{1-x}Mn_xO$ ($x = 0.02$, 0.04 and 0.08) alloys measured at 295 K.

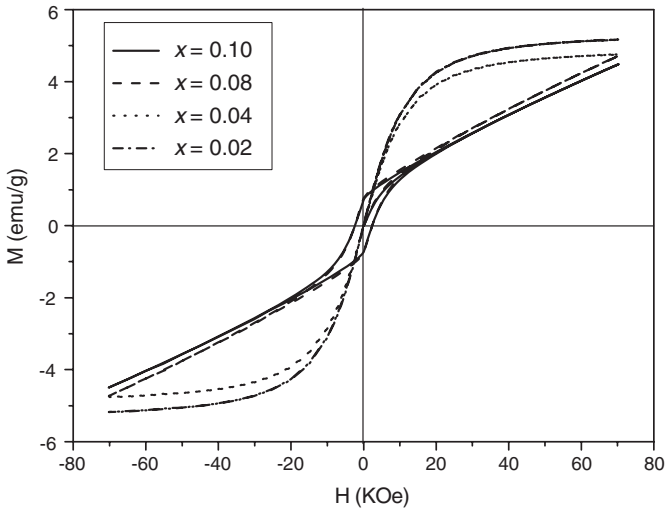

Figure 3. Magnetic moment as a function of external field (M–H) for $Zn_{1-x}Mn_xO$ alloys, samples of $x = 0.02$ and 0.04 measured at 2 K, and $x = 0.08$ and 0.10 at 30 K.

samples exhibited only the Bragg peaks from the wurtzite structure of ZnO (JCPDS No. 80-0075). As for the $x = 0.10$ sample, not only ZnO but also tetragonal Mn_3O_4 (JCPDS No. 80-0382) diffraction peaks were identified, as shown in the inset of figure 1. The linear expansion of the a-axis lattice spacing with an increase in x indicated that doped Mn atoms substitute for Zn atoms in the lattice up to $x = 0.10$. EPR spectra, as shown in figure 2, gave us another proof that Mn^{2+} ions were distributed in the ZnO lattice from the broad EPR line-width caused by the exchange of coupled Mn ions [12, 13].

We ploted the magnetization as a function of magnetic field (M–H) for the samples in figure 3. As can be seen, no hysteresis loops were found for $x = 0.02$ and 0.04 samples even at $T = 2$ K. These two samples were paramagnetic. However, the M–H curves of $x = 0.08$ and 0.10 samples clearly showed hysteresis loops at 30 K. The coercive fields (F_C) and saturation

Table 1. Magnetic properties, Mn concentration, and impurity detected in $Zn_{1-x}Mn_xO$ alloys prepared by the hydrothermal method.

Mn content (x value)[a]	0.002	0.005	0.02	0.04	0.08	0.10
Magnetic properties	PM	PM	PM	PM	FM; PM	FM; PM
Impurity detected	No	No	No	No	Yes (by TEM)	Yes (by XRD)

[a] The 0.002 and 0.005 samples were cited from [13]; the rest were measured in this work. PM stands for paramagnetism; FM for ferromagnetism.

magnetization (M_S) of the two samples were close. The magnetic moments were unsaturated up to 7 T, which indicates that they coexist with the paramagnetic phase.

In order to understand the different magnetic states, we investigated the frequency dependence of ac susceptibility of the samples. Figure 4 is the plot of the real part of χ' as a function of temperature at various frequencies. As for the $x = 0.02$ and 0.04 samples, the three ac susceptibility curves measured at 11, 332 and 997 Hz overlapped entirely. No frequency dependence was observed. A peak with frequency dependence was found for the $x = 0.08$ sample, and thus spin–glass behaviour existed. It was reported that there was a secondary phase when the magnetization versus temperature behaviour showed a spin–glass-type transition [14]. The spin–glass behaviour in the $x = 0.08$ sample gave us a clue that a secondary phase might exist, although it had not been detected by the XRD technique. To confirm the speculation, the high-resolution TEM (HRTEM) technique was applied. In most cases, the alloys were ZnO wurtzite phase from HRTEM and the corresponding SAED pattern, as shown in figure 5(a). Occasionally, nanometre-sized clusters dispersed in $Zn_{1-x}Mn_xO$ alloys were found. The SAED pattern inserted in figure 5(b) demonstrated that the cluster inclusions were in a tetragonal structure. Regarding the cluster inclusions' structure, natural possibilities are the manganese oxide phases, Mn_3O_4 or $(Mn, Zn)Mn_2O_4$ (Zn-doped Mn_3O_4). To further identify the secondary phase, the zero-field cooling (ZFC) and the field cooling (FC) magnetization as a function of temperature (M–T) curves are illustrated in figure 6. The FC data begin to deviate from the ZFC data at around 50 K and the ferromagnetic transition was at $T_C = 39$ K. The transition temperature of Mn_3O_4 is 43 K [15], while the solid solution $(Zn, Mn)Mn_2O_4$ has a lower T_C [16]. The ZFC–FC magnetization curves, together with HRTEM analysis, confirmed the secondary phase as $(Zn, Mn)Mn_2O_4$ in the $x = 0.08$ sample. A similar conclusion was also drawn for the Fe-doped TiO_2 rutile films. Room-temperature ferromagnetism was associated with the formation of a secondary phase Fe_3O_4, rather than a true dilute magnetic oxide semiconductor [17].

The change of magnetic ordering with Mn concentrations of $Zn_{1-x}Mn_xO$ alloys prepared by the hydrothermal method is summarized in table 1. The magnetic exchange interaction in $Zn_{1-x}Mn_xO$ alloys was paramagnetic when $x \leqslant 0.04$. Among these alloys, the $x = 0.002$ and 0.005 samples had been studied elsewhere [13]. In high Mn concentration samples, the appearance of ferromagnetism resulted from the secondary phase. For example, the secondary phase was not detected by XRD for the $x = 0.08$ sample, and the nanoscale ferromagnetic phase was found by careful microscopy studies. A similar phenomenon was also found for Co-doped TiO_2 anatase film [7]. Therefore, one might draw false conclusions only based on substandard materials science such as the XRD or EPR techniques. The correct path may be followed by careful material preparation, detailed materials characterization, transport and magnetic measurements, and theory to allow structure-function relationships to be determined [7, 17, 18].

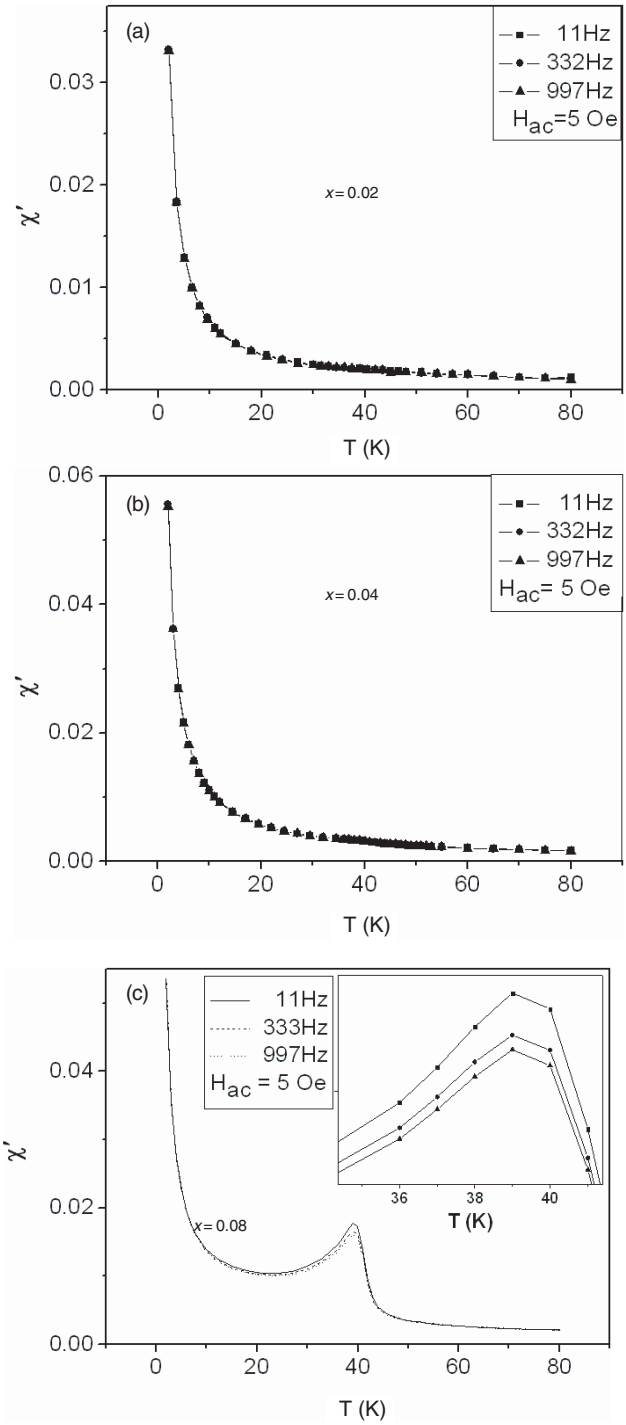

Figure 4. Temperature dependence of the real part χ' of ac susceptibility measured at 5 Oe and 11, 332 and 997 Hz (from top to bottom) for $Zn_{1-x}Mn_xO$ alloys, respectively. The inset in (c) shows the amplifying part of the cusp.

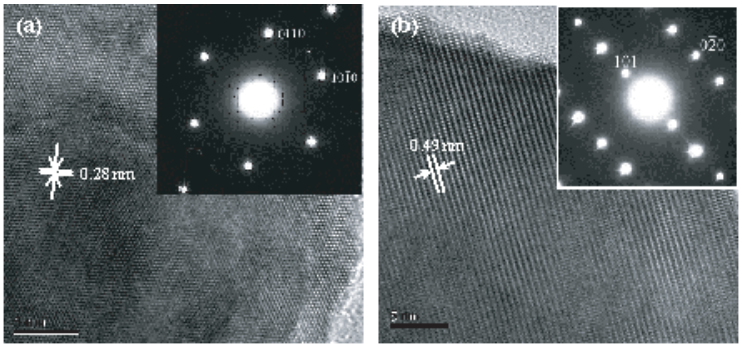

Figure 5. The HRTEM images and the corresponding SAED (inset) of the $Zn_{1-x}Mn_xO$ ($x = 0.08$) alloys (a) and (Zn, Mn)Mn_2O_4 secondary phase (b) in the sample, respectively.

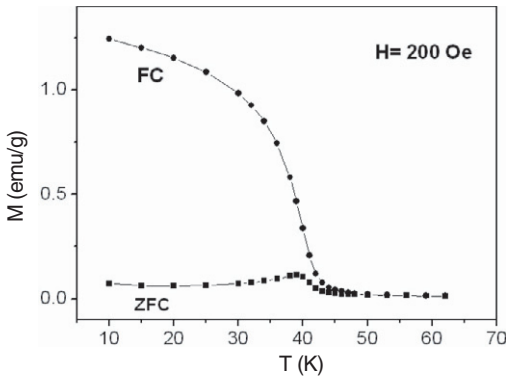

Figure 6. FC and ZFC magnetizations as a function of temperature of $Zn_{1-x}Mn_xO$ ($x = 0.08$) sample in dc applied fields of 200 Oe.

4. Conclusion

In summary, $Zn_{1-x}Mn_xO$ alloys with $x = 0.02$, 0.04, 0.08 and 0.10 were prepared by a hydrothermal method and characterized by several methods. There is no spontaneous magnetization in $Zn_{1-x}Mn_xO$ ($x = 0.02$ and 0.04) alloys. For the $x = 0.08$ and 0.10 samples, it is observed that the ferromagnetism is not due to Mn doping but to the precipitation of a secondary phase, (Zn, Mn)Mn_2O_4.

This work was supported by a grant from the Shanghai Nanotechnology Promotion Center (Project No 0452nm071). The authors thank the referee for valuable suggestions.

References

[1] Furdyna J K 1988 *J. Appl. Phys.* **64** R29
[2] Wolf S A, Awschalom D D, Buhrman R A, Daughton J M, von Molna'r M L, Roukes S, Chtchelkanova A Y and Treger D M 2001 *Science* **294** 1488
[3] Ohno H 1999 *J. Magn. Magn. Mater.* **200** 110
[4] Dietl T, Ohno H, Matsukura F, Cibert J and Ferrand D 2000 *Science* **287** 1019
[5] Fukumura T, Yamada Y, Toyosaki H, Hasegawa T, Koinuma H and Kawasaki M 2004 *Appl. Surf. Sci.* **223** 62

[6] Matsumoto Y, Murakami M, Shono T, Hasegawa T, Fukumura T, Kawasaki M, Ahmet P, Chikyow T, Koshikara S and Koinuma H 2001 *Science* **291** 854
[7] Chambers S A, Droubay T, Wang C M, Lea A S, Farrow R F C, Folks L, Deline V and Anders S 2003 *Appl. Phys. Lett.* **82** 1257
[8] Özgür Ü, Alivov Y I, Liu C, Teke A, Reshchikov M A, Doğan S, Avrutin V, Cho S J and Morkoç H 2005 *J. Appl. Phys.* **98** 041201
[9] Sharma P, Gupta A, Rao K V, Owens F J, Sharma R, Ahuja R, Osorio Guillen J M, Johansson B and Gehring G A 2003 *Nat. Mater.* **2** 673
[10] Kundaliya D C, Ogale S B, Lofland S E, Dhar S, Metting C J, Shinde S R, Ma Z, Varughese B, Ramanujachary K V, Salamanca-Riba L and Venkatesan T 2004 *Nat. Mater.* **3** 709
[11] Shi E W, Chen Z Z, Yuan R L and Zheng Y Q 2004 *Hydrothermal Crystallogr* (Beijing: Science Press)
[12] Schneider E E and England T S 1951 *Physica* **17** 221
[13] Zhang H W, Shi E W, Chen Z Z, Liu X C and Xing B 2006 *J. Magn. Magn. Mater.* **305** 377
[14] Özgür Ü, Alivov Y I, Liu C, Teke A, Reshchikov M A, Doğan S, Avrutin V, Cho S J and Morkoç H 2005 *J. Appl. Phys.* **98** 041201
[15] Norton D P, Pearton S J, Hebard A F, Theodoropoulou N, Boatner L A and Wilson R G 2003 *Appl. Phys. Lett.* **82** 239
[16] Jacobs I S and Kouvel J S 1961 *Phys. Rev.* **122** 412
[17] Kim Y J, Thevuthasan S, Droubay T, Lea A S, Wang C M, Shutthanandan V, Chambers S A, Sears R P, Taylor B and Sinkovic B 2004 *Appl. Phys. Lett.* **84** 3531
[18] Tuan A C, Bryan J D, Pakhomov A B, Shutthanandan V, Thevuthasan S, McCready D E, Gaspar D, Engelhard M H, Rogers J W Jr, Krishnan K, Gamelin D R and Chambers S A 2004 *Phys. Rev.* B **70** 054424